Hierarchical HAC$_\infty$/LAC Vibration Suppression for a Flexible Space Telescope: SPICE

Armando A. Rodriguez
Department of Electrical Engineering
Center for Systems Science and Engineering
Arizona State University
Tempe, AZ 85287-5706

Delano R. Carter *
Department of Electrical Engineering
Center for Systems Science and Engineering
Arizona State University
Tempe, AZ 85287-5706

Abstract

This paper describes the synthesis of a dynamic compensator for a flexible space telescope truss structure described by a 256th ordered finite-element NASTRAN model and 24 disturbance states. The control objective is to attenuate the induced LOS disturbance (jitter) by a factor of 100 over the open loop value. A combination of Low Authority Control (LAC) followed by High Authority Control (HAC$_\infty$) which utilizes the H$_\infty$ optimal control methodology make up the hierarchical control loop design approach for obtaining robust stability and precision performance from the large flexible space telescope truss structure. The LAC loop is made up of two loops which provide broadband modal damping, modal spillover robustness, and actuator mode stabilization all of which help to stabilize the HAC$_\infty$. The HAC$_\infty$ suppress specific targeted modes after LAC loop closing to attain the desired performance level. The HAC$_\infty$ loop controller order is reduced from 130-states to 60-states by applying frequency-weighted balanced truncation techniques to the controller input stability measure. The resulting hierarchical HAC$_\infty$/LAC controller is robustly stable against ±10% variation in actuator and sensor modeling.

1. Introduction

This paper describes a HAC$_\infty$/LAC based control synthesis procedure for the structural control of the Air Force's Space Integrated Controls Experiment (SPICE) which physically resides in the Phillips Laboratory on Kirtland A. F. B. in Albuquerque, New Mexico. This test article is representative of a large precision optical structure. The flexible space telescope truss structure is made of graphite-epoxy and utilizes a tripod configuration in combination with a two-level hexagonal truss used as a primary mirror bulkhead to form a telescope. The structure stands 8 m tall with a 6 m diameter base. The secondary mirrors for the telescope are located at the top of the tripod. The first flexible mode of the telescope is around 7 Hz when fully mass-loaded with dummy primary and secondary mirrors.

* This research has been supported in part by a GEM fellowship and by Honeywell Satellite Systems Operation.

To obtain high quality optical imaging from the telescope, the flexible body modes must be controlled in the presence of disturbance sources. In this way, the induced line-of-sight (LOS) disturbances can be minimized. The LOS disturbances result from structural deformation induced by six disturbance sources. The applied structural disturbances induce an open-loop LOS jitter of 100 μrad root-mean-square (rms) in two orthogonal axes. There are eighteen proof-mass actuators (PMA) distributed about the truss structure to provide the required structural control forces. The disturbance source point of entry to the structure and the actuator locations on the structure prohibit disturbance cancellation at the source. A host of sensors are available for measuring the induced structural deformations.

The control objective is to attenuate the induced LOS disturbance (jitter) by a factor of 100 over the open loop value. A hierarchical HAC_∞/LAC loop design approach was undertaken to achieve the desired LOS disturbance rejection with the H_∞ optimal control designed HAC_∞ loop providing the necessary performance required. The sensors utilized for feedback to the structural controller are complementary collocated accelerometers located at each PMA and PMA linear variable differential transformer (LVDT) signals which provide proof mass displacement information. The accelerometers are attached to the PMA housing which are in turn attached to the flexible structure. Thus, the accelerometers yield a measure of the local structural acceleration at the PMA attach points. The LVDT located within each PMA provides a measure of the relative displacement between the PMA housing and its proof mass. For this active structural control design, the LOS signals weren't fedback. The structural controller described in this paper achieves the control objective in the absence of significant actuator/sensor noise levels.

2. Plant Model Description

In this section, a more detailed description of the SPICE hardware and models are given.

2.1 Truss Structure

The truss structure has a three sided pyramid shape with struts made of graphite-epoxy. It measures 8 meters tall and 6 meters wide at the hexagonal base diameter. A diagram of the structure is given in Figure 1. The number of struts and node balls making up the truss structure is listed in Table 1.

Figure 1. Telescope Truss Structure With Disturbance
and Actuator Locations

Table 1. Telescope Truss Structure Statistics

Number of Struts (Including Tripod Legs):	264
Number of Node Balls:	64
Loaded Mass (kg)	2700

A dummy primary mirror is attached to the top of the bulkhead and a dummy secondary mirror attached to the top of the tripod. To induce structural vibrations, six disturbance forces are applied to the truss structure. Three disturbance forces are located at the top of the truss structure where the secondary mirror for the telescope would be located. These disturbances will be referred to as secondary mirror disturbances throughout this paper. A secondary mirror disturbance is applied to each tripod leg and is active in three orthogonal translational axes. The secondary mirror disturbance forces are generated by shakers with output forces sized to yield about half of the 100 μrad rms LOS disturbance.

The three other disturbance forces are located at the base of the telescope truss structure. These disturbances will be referred to as base disturbances. There is one base disturbance acting at each vertex of the hexagonal shaped lower bulkhead. These disturbances are generated by an active isolation system located beneath the telescope. These disturbances act primarily in the vertical direction (z coordinate) and are sized to be the source of the other half of the 100 μrad rms LOS disturbance. All disturbances are generated by coloring unit intensity white Gaussian noise with a bandpass coloring filter with 2^{nd} order poles at 5 Hz and 10 Hz. These filters are then scaled to generate the desired rms force levels. Their location on the truss structure illustrated in Figure1. The power spectral density (PSD) of the disturbance filters is given in Figure 2.

Figure 2. Disturbance Power Spectral Density

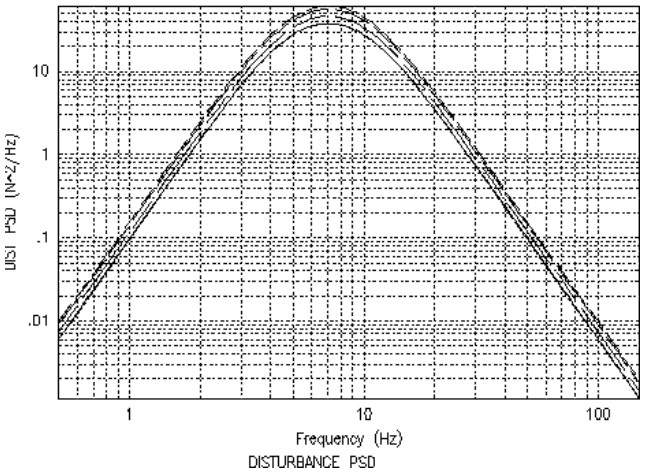

The flexible telescope structure is instrumented with an optical scoring system (OSS) which combines translational and rotational structural deformation sensor information to yield a LOS disturbance measure in two orthogonal directions (x and y rotations). The OSS sensor output are available for control feedback but weren't used in this controller design. The open loop LOS disturbance as measured by the OSS due to the secondary mirror and base disturbances is 100 μrad rms in x and y rotation. Shown in Figure 1 is a diagram showing the optical beam path for the OSS.

2.2 Actuator Description

Structural control forces are provided by eighteen (18) PMA that are distributed about the telescope structure (see Figure 1). Each PMA has an integral linear accelerometer mounted to its housing thus providing a complementary collocated acceleration signal. Each PMA also has a LVDT which senses the relative displacement between the PMA housing and the PMA proof mass. Six of the PMAs are located at the lower bulkhead hexagonal vertices and act in the vertical (z-) direction. The other twelve PMAs are located on the tripod legs. Each tripod leg has two (2) pair of PMAs attached. One pair is located about a third from the top of the tripod leg and the other pair is about two thirds from the top of the tripod leg. Each pair of PMAs on the tripod legs act in orthogonal directions to each other and normal to the tripod leg. An illustration of the PMA attach points on the truss structure is given in Figure 1.

A PMA force command is scaled to produce a PMA coil current command. This current command is applied to the current loop which generates the desired current in a coil of wire wrapped around a core which is attached to the PMA housing. This current flow is established in a magnetic field generated by permanent magnets which are supported by flexures (the proof mass). The flexures are attached to the

PMA housing. The interaction of the current flow and the magnetic field generates a force perpendicular to each and in the direction of the PMA core. As a result of this interaction, equal and opposite forces are applied to the proof mass and the PMA core. At higher frequency, the force applied to the PMA core is transmitted to the truss structure via the PMA housing thereby providing structural control forces. Also at the higher frequencies, the force applied to the proof mass is isolated from the truss structure by the flexure suspension. The proof mass and its flexure suspension stiffness and combine to create a lightly damped resonance around 5 Hz when the PMAs are attached to the truss structure. The PMA behaves as a second order bandpass filter from commanded force to applied force. The lower break frequency is around 5 Hz and the upper break is set by the current loop bandwidth and is around 2 kHz. The assumed noise PSD for each PMA is white in the frequency range of interest with an amplitude of 0.03 N^2/Hz.

2.3 Sensor Description

The sensor inputs used in this controller design consists of differentiated LVDT signals and integrated PMA accelerometer signals. The LVDT and accelerometer sensors are assumed ideal. The assumed integrated accelerometer noise PSD is white in the frequency range of interest with an amplitude of 0.05 mm^2 per sec^2/Hz.

2.4 Structural Finite-Element Model Description

Results from a MSC/NASTRAN finite-element model of the telescope truss structure including the PMA were used for active structural control synthesis. Some NASTRAN model statistics are given in Table 2. The NASTRAN model yielded 128 flexible modes (256 states) below 150 Hz. The lowest mode of the telescope truss structure excluding PMA modes occurs around 7 Hz. All modes are lightly damped with damping ratios (ζ) on the order of 0.007. The mode with the smallest damping ratio is at 8.7 Hz with a value of 0.0009. Four of the LOS significant flexible body mode shapes of the telescope are shown in Figure 4. The NASTRAN model inputs were secondary mirror and base disturbances, and PMA force commands. Outputs from the model were OSS LOS x and LOSy measurements, PMA attach point integrated acceleration (velocity) in the direction of the PMA line of action, and the PMA relative displacement rate between the PMA housing and proof mass (differentiated LVDT signal). The NASTRAN model results were used to create a modal space model of the truss structure which was used for the structural controller design.

The open loop LOS disturbance PSD and backsum plots are illustrated in Figures 5 & 6. The resultant LOSx is 93.4 μrad rms and LOSy is 92.7 μrad rms . The disturbance sources were sized to provide the 100 μrad rms value to the telescope truss structure LOS without PMAs attached. The open-loop singular value plot from PMA force command to integrated accelerometer outputs is shown in Figure 7.

Table 2. NASTRAN Model Statistics

Nodes:	2534
Bar Elements:	2220
Plate Elements:	1527
Solid Elements:	48
Spring Elements:	135
Rigid Elements:	55
Concentrated Mass Elements:	194
Total Elements:	4179
Analysis Degrees of Freedoms:	13398
Scalar Degrees of Freedoms:	2
Total Mass (kg):	2840
Modes below 150 Hz (including rigid)	134

Figure 4. Four Optically Significant Flexible Modes

Figure 5. Open Loop LOS PSD

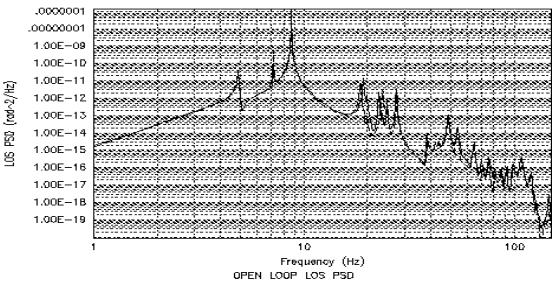

Figure 6. Open Loop LOS RMS Backsum

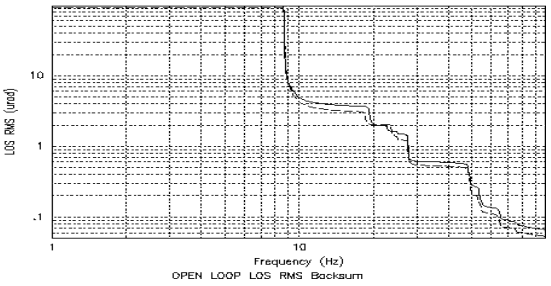

Figure 7. Proof Mass Actuator Inputs to Integrated Accelerometer Outputs Open Loop SV Plot

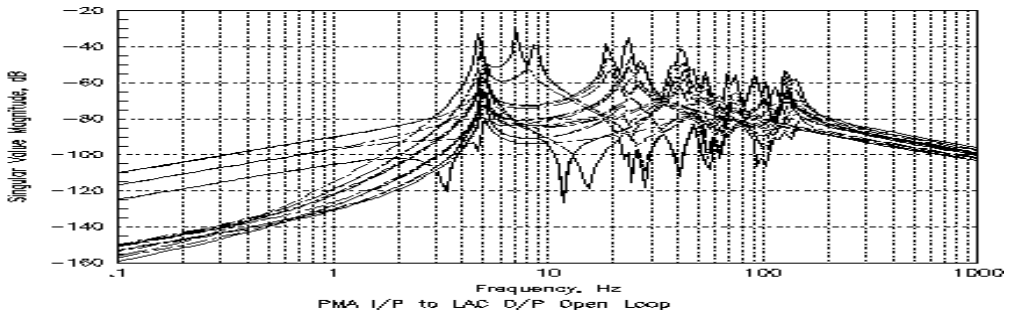

The plant model consists of a graphite-epoxy telescope truss structure with six disturbance forces, an OSS to measure LOS disturbances, eighteen PMAs to provide structural control forces, eighteen linear accelerometers collocated with the PMAs to provide structural acceleration sensing at the PMA locations, and eighteen LVDT measurements sensing the relative displacement between the PMA housing and proof mass.

3. Description of Hierarchical HAC$_\infty$/LAC Control Design Methodology: Application to SPICE

A hierarchical HAC$_\infty$/LAC approach to structural controller synthesis was undertaken to develop a controller which would satisfy the factor of 100 LOS jitter reduction control objective. This approach consisted of sequentially closing three loops each designed to meet some specific control objective. The three loops in order of closing are referred to as (1) PMA damping loop, (2) local rate feedback, (3) high authority control loop. The HAC$_\infty$/LAC control system block diagram is given in Figure 8.

Figure 8. HAC∞/LAC Control System Block Diagram

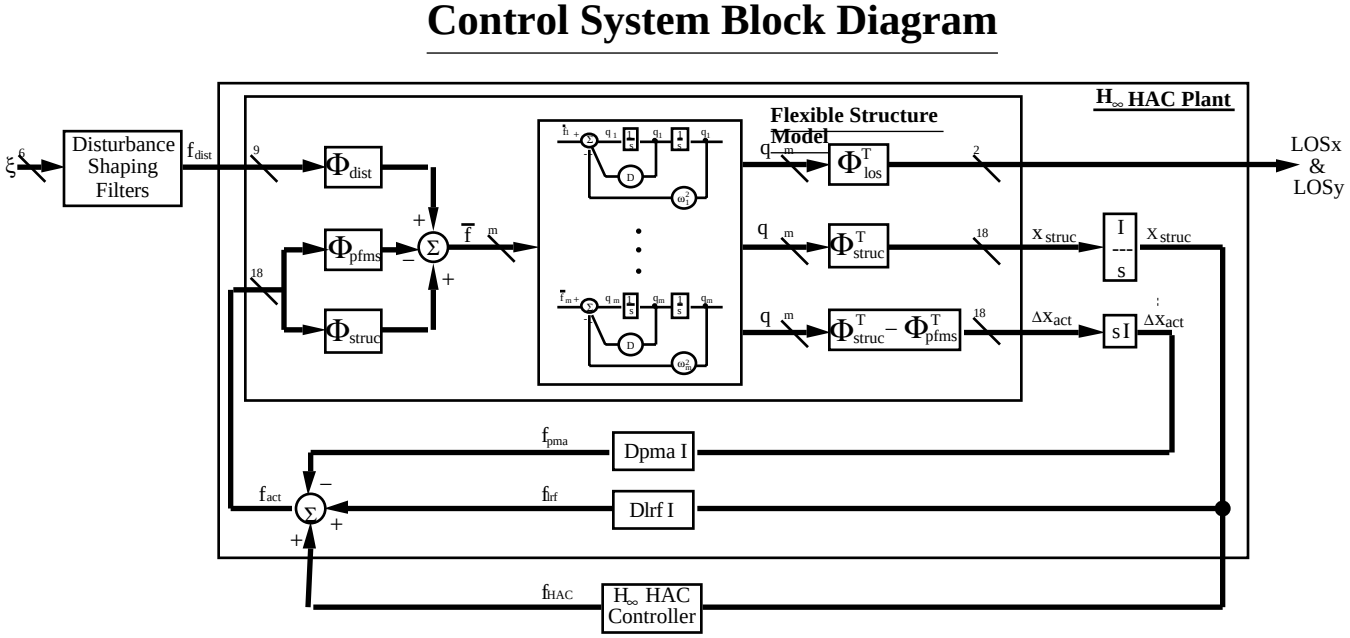

3.1 Low Authority Controller

The PMA damping and local rate feedback loops are collectively referred to as the low authority control. Low authority because these loops provide broadband damping to structural vibrations using rate information rather than attacking specific troublesome modes which contribute significantly to LOS jitter. The LAC loop will be implemented analog to keep the sample rates low.

3.1.1 PMA Damping Loops

The initial controller design consists of providing damping to the 5 Hz PMA modes. Local damping of these modes is achieved by differentiating the LVDT signal to get a measurement of the rate at which the proof mass is changing with respect to (wrt) its housing, scaling this measurement, and feeding it back to the respective PMA as a force command. The PMA damping loop design had two control objectives. To provide damping to the PMA mode while at the same time reducing the induced rms LOS disturbance. A scale factor of 220 N/m per s for each PMA damping loop achieved the best compromise between the two control objectives. Too much or too little PMA damping permitted more LOS jitter relative to this value of damping. The resultant LOS PSD and backsum plots with the PMA damping loops closed are shown in Figures 9 & 10. The resultant rms LOSx and LOSy is 14.7 µrad rms and 13.8 µrad rms, respectively.

Figure 9. LOS PSD With PMA Loops Closed

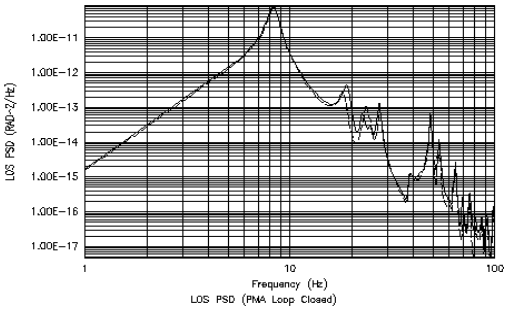

Figure 10. LOS Backsum With PMA Loops Closed

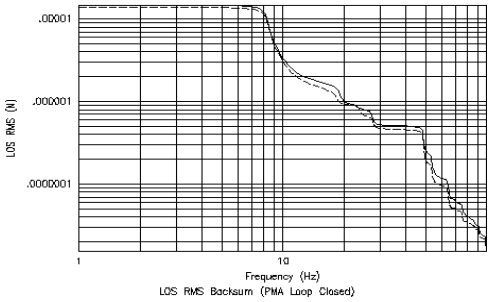

3.1.2 Local Rate Feedback

Having closed the PMA damping loop, the local rate feedback (LRF) loop controller is designed. To increase stability robustness against spillover modes and to provide structural damping, each PMA housing accelerometer is integrated, scaled, and fed back as a force command to the respective PMA. The integrated housing accelerometer yields a measure of structural rate of change wrt fixed space at each PMA location. Since the telescope truss structure rigid body has no net acceleration, the measured motion must be due to flexible body vibrations. The objective for the LRF loop is to minimize the rms LOS disturbance and maintain satisfactory stability margin. Due to right half plane transmission zeros from PMA force commands to integrated housing accelerometer outputs, there exists an upper limit on how much rate feedback may be applied. The upper limit was determined to be at 2200 N per m/s. At this level of LRF, the structure eigenvalues moved into the right half plane. To satisfy the control objectives for the LRF loop, a value of 1000 N per m/s was used.

The resultant PSD and backsum plots with the low authority control loop closed is given in Figures 11 & 12. The resultant LOS disturbances are 8.6 µrad LOSx and 8.0 µrad LOSy.

3.2 High Authority Controller

The final loop to be closed in this hierarchical HAC_∞/LAC control loop design is the H_∞ HAC loop. The objective for the HAC_∞ loop is to reduce the residual LOS disturbance after LAC loop closing to about 1 µrad rms by controlling specific modes which contribute significantly to the LOS jitter. The design plant block diagram used for H_∞ HAC controller synthesis is given in Figure 13.

Figure 11. LOS PSD With LAC Loops Closed

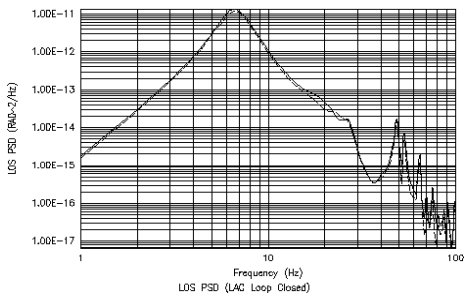

Figure 12. LOS Backsum With LAC Loops Closed

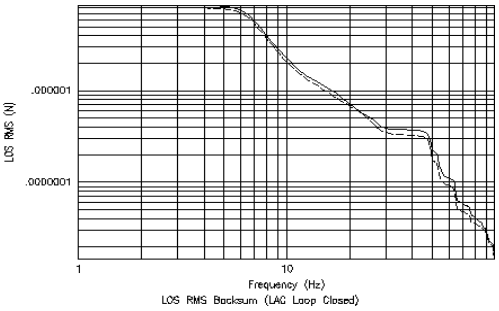

Figure 13. HAC Design Plant for H_∞ Controller Synthesis

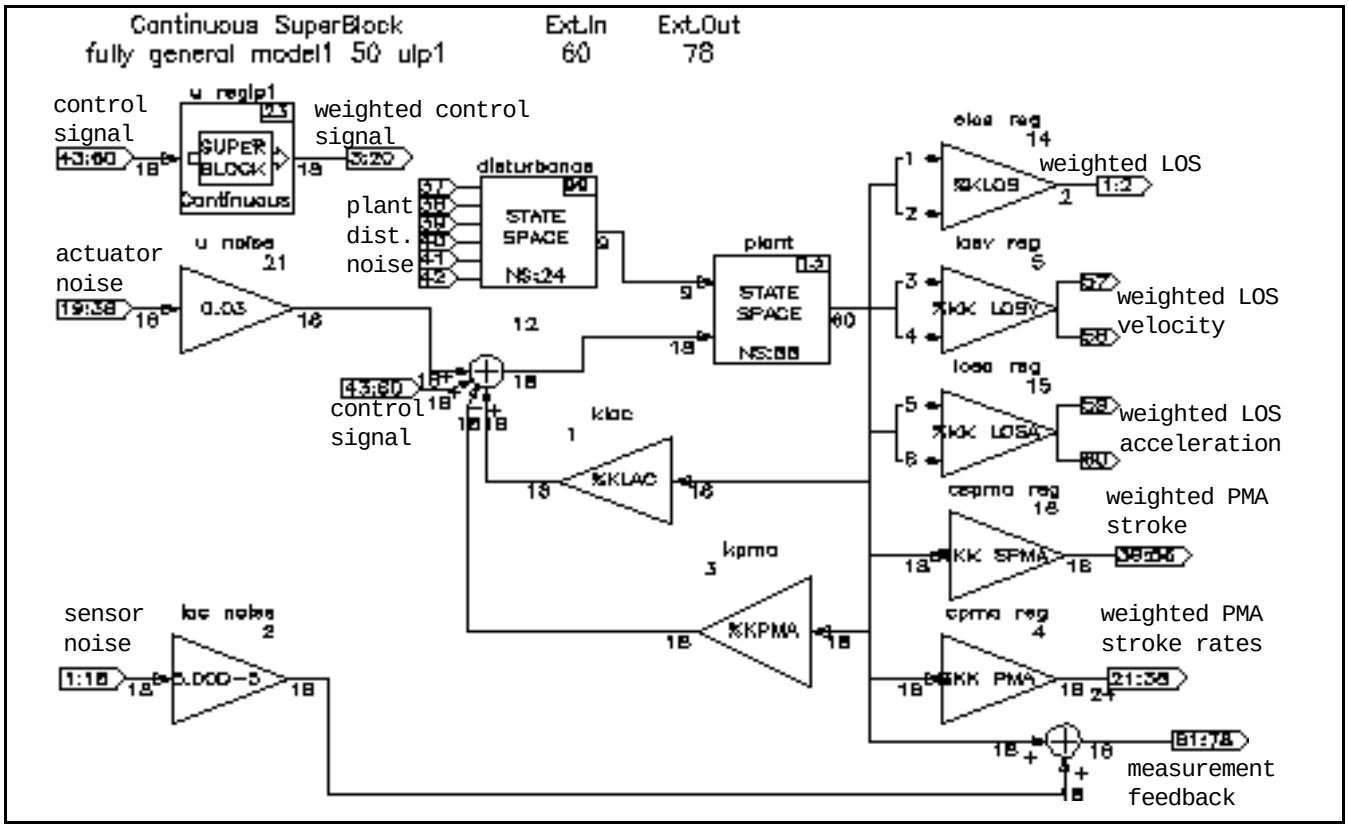

The feedback to the H_∞ designed controller is the integrated accelerometer outputs (measurement feedback) so feedback of the regulated signal wasn't utilized. For determination of which modes to attack to satisfy the performance objective, the modal model LOS outputs were weighted in the design plant. This provided the HAC controller the information of which modes were causing the most LOS disturbance and therefore which modes to control. The plant was determined to be controllable and

stabilizable from the PMA force command inputs to the integrated PMA accelerometer outputs. This satisfies an important condition for the existence of a stabilizing H_∞ controller. The singular value plot from the PMA force command inputs to the integrated PMA accelerometer outputs with LAC loop closed is shown in Figure 14.

Figure 14. Proof Mass Actuator Inputs to Integrated Accelerometer Outputs With LAC Loop Closed

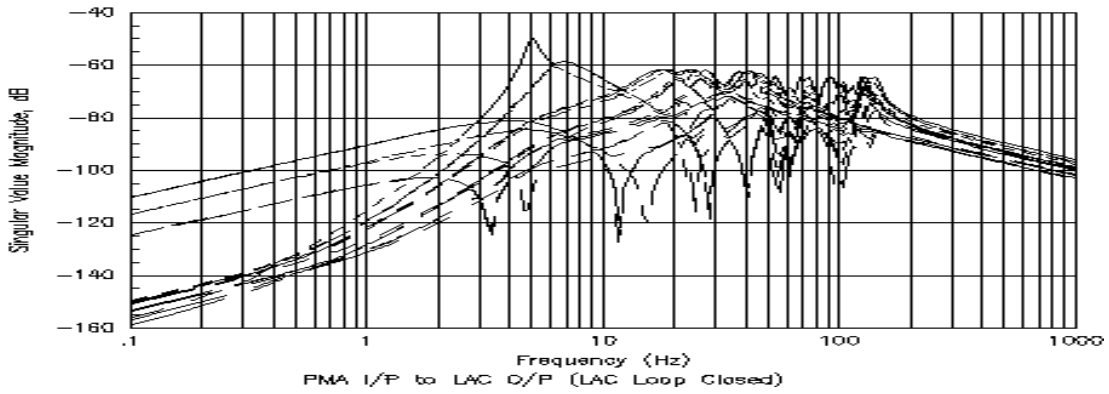

The LOS weighting function essentially applies a cost penalty on state deviation from null which is to be minimized by the H_∞ designed controller. To reduce the HAC_∞ closed loop bandwidth and the compensator order, all flexible modes above 55 Hz were truncated from the modal model. This resulted in maintaining the 18 PMA modes plus 26 flexible modes in the design plant model. A frequency dependent weighting function was applied to the PMA force command to limit the actuator control authority and system closed loop bandwidth. As seen in the design plant model, various signals were weighted but weighting on the LOS, control input, and PMA stroke rate signals yielded the best results. The set of control/sensor weighting functions which achieved the desired performance objective is shown in Table 3. The design plant totaled 130 states (88-flexible modes; 24-disturbance shaping filters; 18-PMA control weighting function) which resulted in a H_∞ HAC compensator of the same order. The resultant compensator singular value plot is given in Figure 15. The resultant LOS jitter using the full up modal model (128 flexible modes; 280 states including disturbance shaping filter) is 1.02 µrad rms in the x-direction and 1.03 µrad rms in the y-direction.

Table 3. Control/Sensor Weighting Functions

LOSx/LOSy	$20 \times 10^6 / 23 \times 10^6$
Differentiated LVDT signal	200
PMA HAC command	$\frac{\frac{s}{2\pi 5}+1}{8.5\left(\frac{s}{2\pi 5000}+1\right)}$
All other signals	0.0

Figure 15. 130 State HAC∞ Controller SV Plot

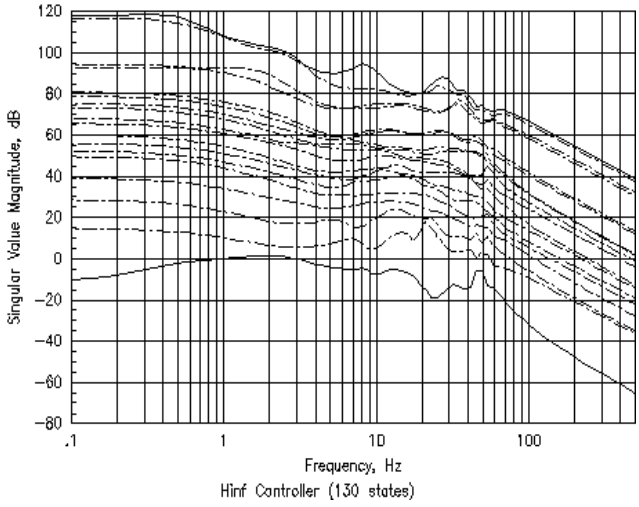

The 130 state HAC∞ compensator was reduced to a 60 state HAC∞ compensator by applying frequency-weighted balanced truncation to the error measure

$$\left\| [C - C_r] P \left[I + CP^{-1} \right] \right\|_\infty$$

which results in a stabilizing reduced order compensator C_r when the compensator C stabilizes the plant P and the error measure is less than 1. This error measure attempts to maintain the compensator input stability margin (loop broken at compensator input) using a reduced order controller. The Hankel singular values associated with the 130 state compensator is given in Figure 16. The 60 state HAC∞ compensator singular value plot is given in Figure 17. The resultant LOS PSD and backsum plots using the full up modal model (128 flexible modes; 280 states including disturbance shaping filter) and the reduced order HAC∞ controller are given in Figures 18 & 20. The resultant residual LOS jitter is 1.02 μrad rms in the x-direction and 1.04 μrad rms in the y-direction. These values are about the same as for the 130-state compensator indicating that compensator order reduction by more than 50% yields minimal impact on performance.

Figure 16. 130 State HAC∞ Controller Hankel Singular Values

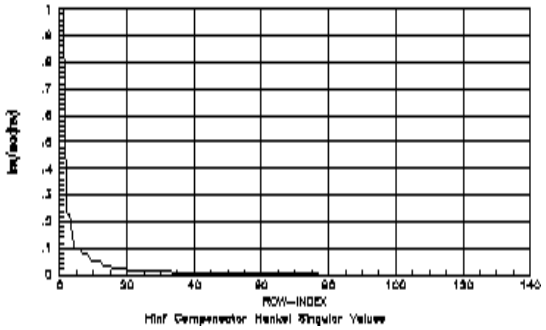

Figure 17. 60 State HAC∞ Controller

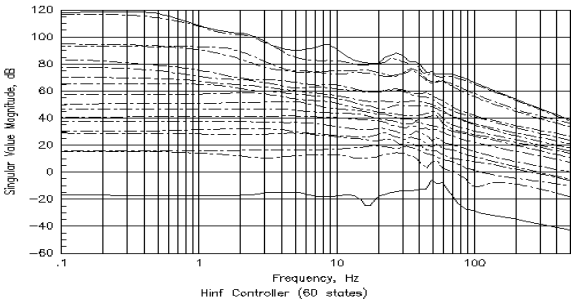

Figure 18. LOS PSD With HAC∞/LAC Loops Closed

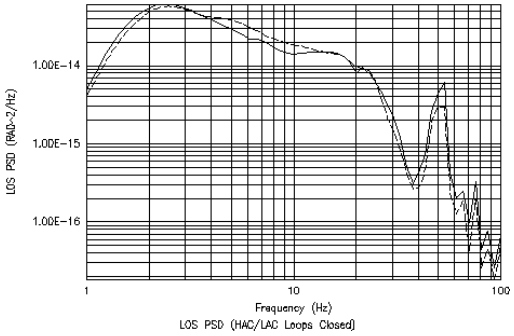

Figure 19. LOS Backsum With HAC∞/LAC Loops Closed

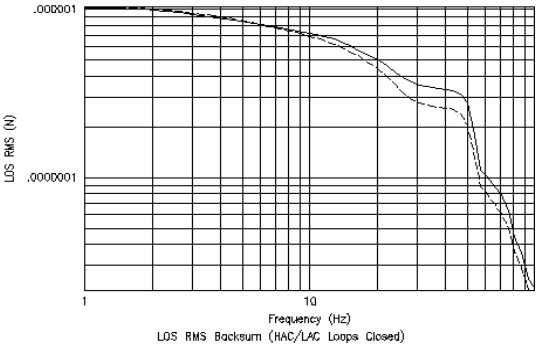

4. Simulation Results

A linear simulation was used to look at closed-loop frequency responses and time domain results. The closed loop sensitivity and complementary sensitivity singular value plots at the plant input and the plant output are given in Figures 21-24. The stability robustness was tested by including 10% modeling uncertainty into each PMA and PMA integrated acceleration output. The resultant stability margin plot is given in Figure 20. Since the plot remains above 0 dB, robust stability is attained for the 10% modeling uncertainties on actuators and sensors. A PSD and backsum plot is listed for the PMA force and stroke requirement in Figures 25-28. The peak PMA force and stroke for any actuator is 7.7 N rms and 0.9 mm rms. The smallest closed loop damping ratio is 7.045×10^{-3} as compared to the open loop value of 9×10^{-4} indicating better overall system modal stability. The LOS time domain results for the open and closed loops are given in Figures 29 & 30.

Figure 20. Stability Margin Plot

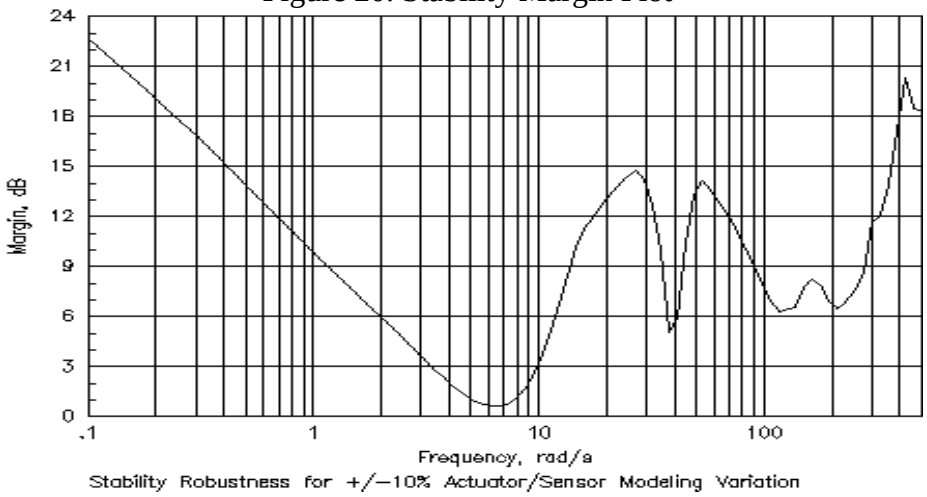

Figure 21. Closed Loop Sensitivity @ Plant Input

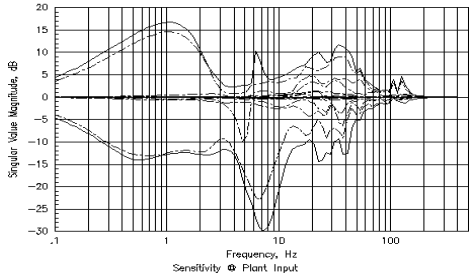

Figure 22. Closed Loop Complementary Sensitivity @ Plant Input

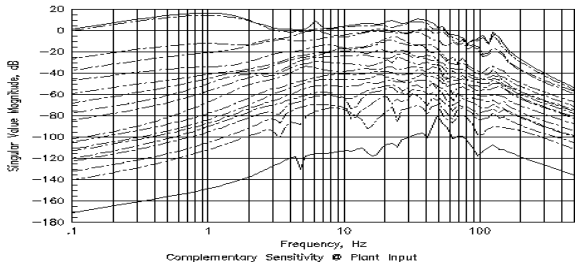

Figure 23. Closed Loop Sensitivity @ Plant Output

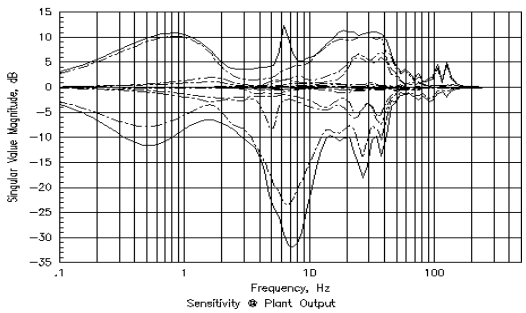

Figure 24. Closed Loop Complementary Sensitivity @ Plant Output

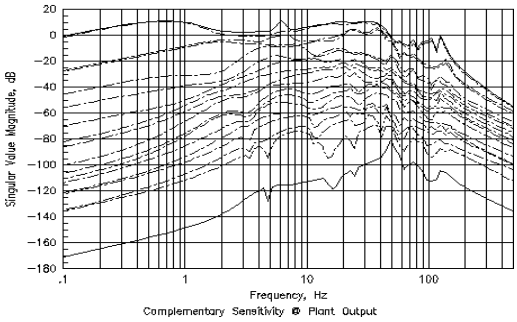

Figure 25. Closed Loop PMA Force PSD

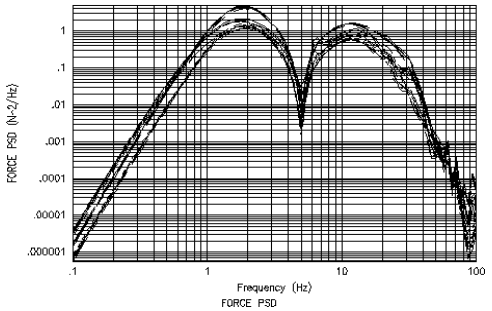

Figure 26. Closed Loop PMA Force Backsum

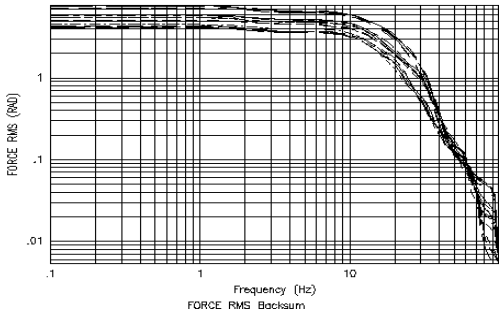

Figure 27. Closed Loop PMA Stroke PSD

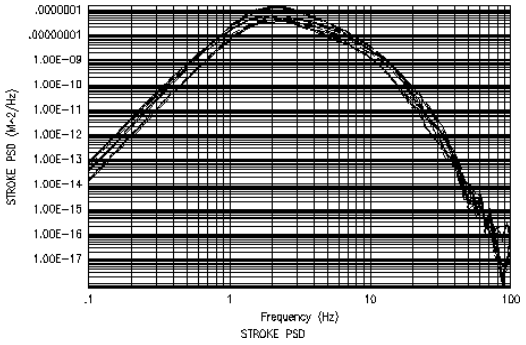

Figure 28. Closed Loop PMA Stroke Backsum

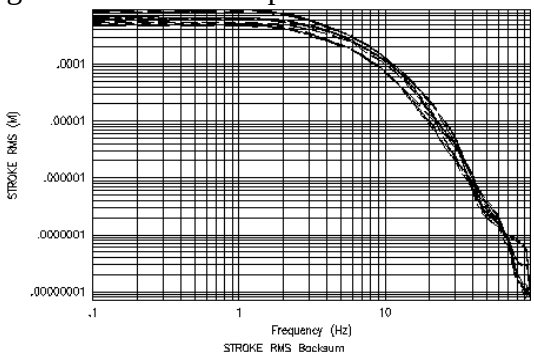

Figure 29. Open Loop LOS Time Responses

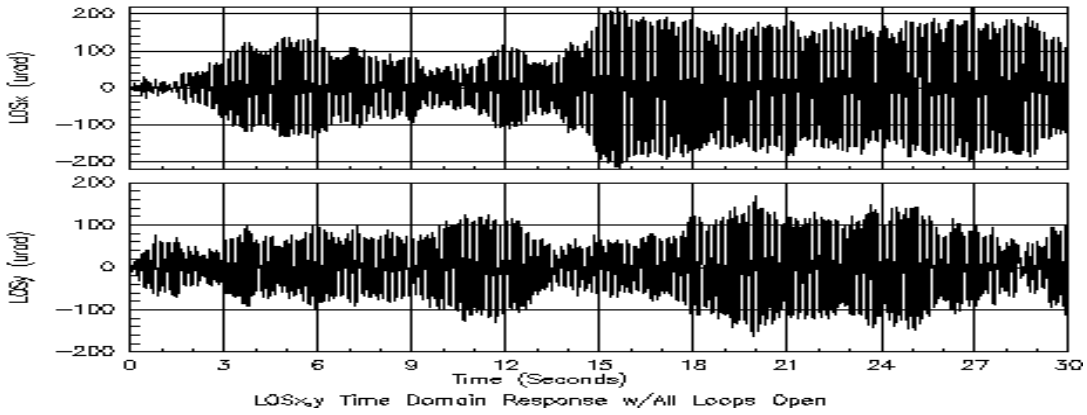

Figure 30. Closed Loop LOS Time Responses

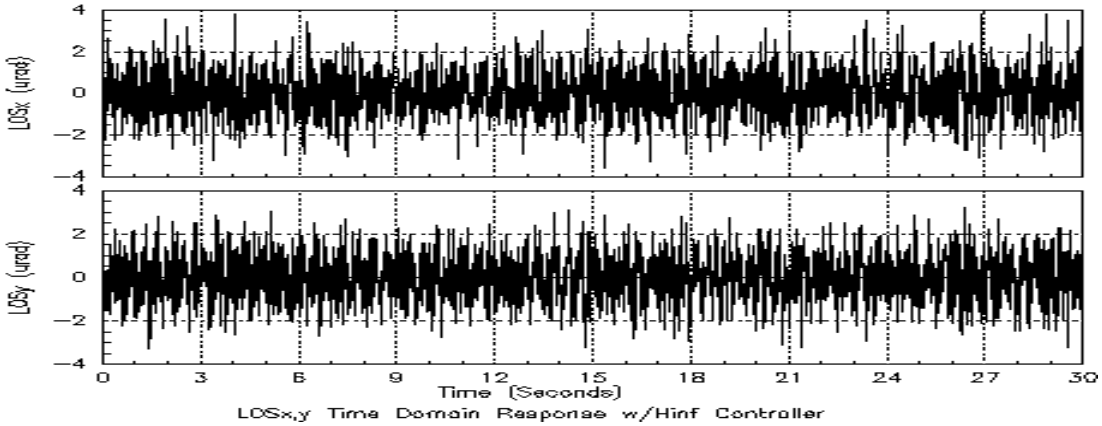

Figure 31. Closed Loop PMA Force and Stroke Time Responses

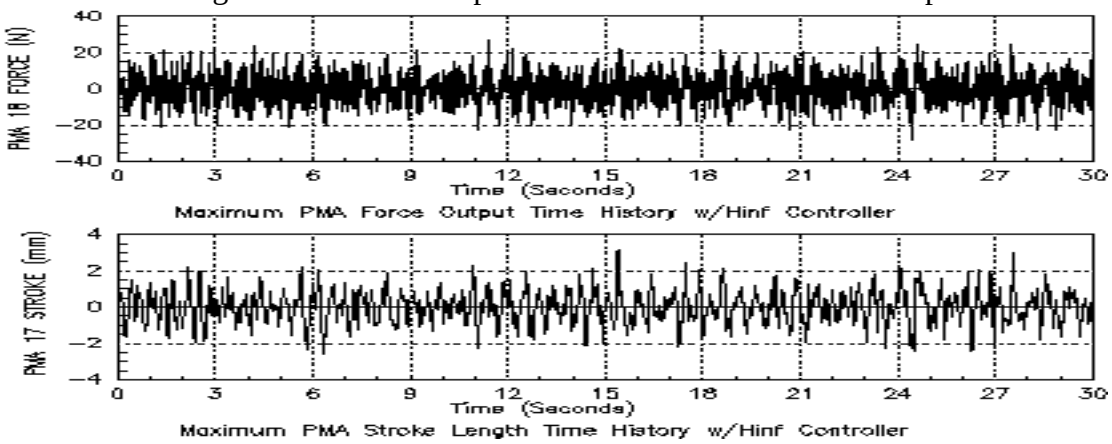

5. Summary and Directions for Future Research

An hierarchical HAC∞/LAC control design has been described for obtaining robust stability and precision performance for the SPICE test article. The combination of H∞ optimal techniques used for High Authority Control (HAC∞) design, to provide the required performance, and Low Authority Control (LAC) methods, which provides additional damping to the structure, achieves a factor of 91.4 LOSx attenuation and 87.9 LOSy attenuation. The structure modal model consisted of 128 evenly distributed flexible modes in the frequency range from 7 Hz up to 150 Hz. The disturbance sources and control actuators were displaced from one another thereby preventing disturbance cancellation at their point of entry to the structure. The passband for the HAC∞ is from .1-50 Hz. The maximum PMA force and stroke is 7.7 N rms and 0.9 mm rms. The resulting hierarchical controller has stability robustness against ±10% variation in actuator and sensor modeling. The LAC loop consisted of two loops which provided actuator stabilization and modal spillover robustness by providing broadband modal damping. Transmission zeros in the right half plane limited the amount of LAC that could be applied thus

limiting the amount of modal damping which could be applied. The HAC$_\infty$ efforts were concentrated on controlling specific modes which still resulted in significant LOS jitter after LAC loop closing. The H$_\infty$ optimal controller used for HAC$_\infty$ was reduced from 130 states to 60 states by applying frequency-weighted balanced truncation techniques on the controller input stability measure. With the LAC and HAC$_\infty$ loops closed, the LOS was reduced from 93.2/91.4 μrad rms in x and y rotation, respectively, to 1.02/1.04 μrad rms using the 60-state HAC$_\infty$ compensator and the 280-state telescope truss structure modal model.

Future research efforts will include studying the effects of actuator nonlinearities, such as saturation, on active structural controller performance, applying other advanced control strategies to the SPICE test article, such as L1 optimal control, developing a set of ordinary differential equations describing the SPICE test article for study in an infinite dimensional setting, and fast LOS stabilization after telescope rapid repointing

References

[1]Safonov, M.G., Chiang, R. Y., and Flashner, H.,"H$^\infty$ Robust Control Synthesis for a Large Space Structure," *Journal of Guidance and Control*, Vol. 14, No. 3, 1991, pp. 513-520.

[2]Balas, G. J., Lukich, M., Dailey, R. L., Doyle, J. C.,"Robust Control of a Truss Experiment," *Proceedings of the American Control Conference*, Atlanta, GA, June 1988, pp. 245-252.

[3]Francis, B. A., and Doyle, J. C.,"Linear Control Theory with an H$_\infty$ Optimality Criterion," *Journal of Control and Optimization* , Vol. 25 No. 4, 1987, pp. 815-844.

[4]Glover, K.,"All Optimal Hankel Norm Approximations of Linear Multivariable Systems and Their L$^\infty$ Error Bounds," *Proceedings of the American Control Conference*, Seattle, WA, 1986.

[5]Aubrun, J. N.,"Theory of the Control of Structures by Low-Authority Controllers," *Journal of Guidance and Control*, Vol. 3, No. 5, 1980, pp. 444-451.

[6]Doyle, J. C., Glover, K., Khargonekar, P. P., and Francis, B. A., "State-Space Solutions to Standard H$_2$ and H$_\infty$ Control Problems," *IEEE Transactions on Automatic Control*, Vol. 34, No. 8, 1989, pp. 831-847.

[7]Hurty, W. C., and Rubinstein, M. F., *Dynamics of Structures*, Prentice-Hall, New Jersey, 1964, Chap. 8.

[8]Thomson, W. T., *Theory of Vibrations with Applications*, Prentice-Hall, New Jersey, 1988, Chap. 6.

[9]Schaeffer, H. G., *MSC/NASTRAN Primer:Static and Normal Modes Analysis*, Schaeffer Analysis, New Hampshire, 1979, Chap. 13.